

On Thermal Drift in a Double Well Aquifer Thermal Energy Storage System

Emma Lepinay¹ and Andy Woods¹

¹Institute of Energy and Environmental Flows, University of Cambridge, Madingley Road, Cambridge CB3 0EZ, UK

el547@cam.ac.uk

Keywords: Aquifer thermal energy storage systems, Thermal imbalance, Heating and cooling systems, Ground-source heat pumps

ABSTRACT

Aquifers can be used to store thermal energy, either produced as waste heat or captured during cooling in summer. This thermal energy can be used for heating in the winter via a heat pump system. Typically, such a system will have an injection and an extraction well, and the flow is reversed seasonally as the system changes from heat storage to heat supply. Here, we present a simplified model to examine the controls on (i) the temperature contrast which develops between the two wells and also (ii) the drift in the temperature of the system if, over a series of years, the heat supply does not match the heat load on the system. We consider the implications of these results in practice.

1. INTRODUCTION

Aquifer Thermal Energy Storage (ATES) systems can contribute to the decarbonisation of space heating and cooling. They provide a source of thermal energy for heating systems, operated by heat pumps, and a reservoir where cooling systems can reject excess thermal energy. Often, these dual-purpose systems have two wells: one for heating in the winter and one for summer cooling. During the summer, water is pumped from a “cold” aquifer to the surface and used as a heat sink for building cooling systems. Cooling the buildings heats the working fluid stored in a “hot” aquifer. In winter, the system is run in reverse; water is pumped from the hot aquifer, and the thermal energy is extracted for space heating. As such, the working fluid is cooled and returned to the cold aquifer, completing the cycle. This operational mode generates an asymmetry in temperature between the two reservoirs, leading to more efficient heating and cooling and enhancing the system's performance.

Oslo Airport is an example of an ATES system which can fully meet its cooling demand in the summer and 30% of its heating demand in the winter (Eggen and Vangnes 2005). However, data collected from a number of different multi-well sites indicate a net drift in the thermal energy of the overall system (Fleuchaus et al. 2020; Sommer, Doornenbal, et al. 2013; Willemsen 2016; Bonte et al. 2011). An imbalance in demand can accumulate over many years and lead to sub-optimal performance of the full system. These reservoirs can be operated sustainably, but controls are necessary to mitigate the effects of a mismatch between heating and cooling demand.

Earlier models of ATES systems have focused on recovery efficiency, defined in terms of the ratio of the extracted energy to the energy injected into a single well (Doughty et al. 1982; Bloemendaal and Hartog 2018; Bödvarsson and Tsang 1982). These studies have identified how, due to thermal diffusion, dispersion and background flow, thermal energy is lost to the surrounding impermeable rock over multiple cycles (Schout et al. 2014; Sommer, Valstar, et al. 2013; Bloemendaal and Olsthoorn 2018). They have also demonstrated the impact of the aquifer geometry on this recovery efficiency: in particular, the thermal efficiency depends on the ratio of (a) the length scale associated with the ratio of the volume to the surface area of the injected fluid to (b) the length scale of thermal diffusion over an injection period (Doughty et al. 1982; Bloemendaal and Hartog 2018).

Using the conservation of heat, we build on the previous work and develop a reduced-order model to explore the behaviour of a double-well ATES system. The paper focuses on the temperature evolution in the hot and cold reservoirs when there is a systematic imbalance between the heat supply and heat demand. This leads to a more complex thermal evolution of the system. We analyse the effects of the aquifer properties and ratio of heating to cooling to gain insight into the controls on the system's performance. In section (3.1), we establish the characteristics of a system running in equilibrium. In section (3.2), we explore the effect of a mismatched cyclic heating and cooling demand over a period of years and observe a net cooling of the full system. We consider the implications of these results for the design and practical operation of the ATES system and draw some conclusions.

2. MODEL

To analyse some of the basic mechanisms in a double-well ATES, we model the working fluid in the hot and cold aquifers and the rock surrounding the injection fluid. The system is operated in a cyclical pattern associated with the seasonal change in demand. During the summer, fluid from the cold well is extracted to provide space cooling. The process of cooling a building allows the fluid to gain thermal energy. This exchange happens at the heat pump and can be modelled by a fixed increase in the temperature ΔT_s of the fluid. The warmer fluid is subsequently pumped into the hot well, where it is stored until the winter season. In our idealised model, after six months, the system is operated in reverse to provide space heating. The fluid is extracted from the hot well and cooled by a fixed temperature ΔT_w ; subsequently this fluid is injected into the cold well.

The thermal mass of the working fluid, injected and extracted from each aquifer, is modelled by $M_f = \rho c_p T_f V_f$ where T_f is the temperature of the fluid, V_f the volume of the fluid, ρ the density, and c_p the specific heat capacity of the fluid. There is a region of rock,

surrounding and in thermal contact with the working fluid, which is modelled by the thermal mass M_r . This thermal mass is defined as $M_r = \rho_r c_p T_r V_r$ where T_r is the temperature of this region of rock, ρ_r the density, and c_{pr} the specific heat capacity of the rock.

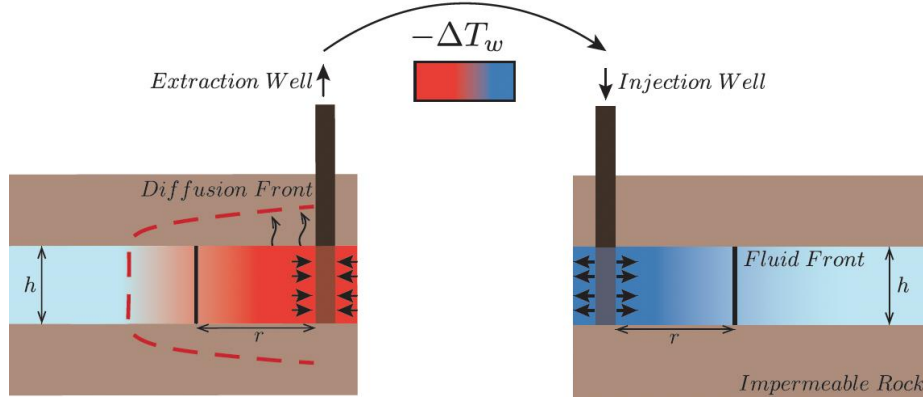


Figure 1: Schematics of the ATES double-well model operating inter-seasonally. The diagram shows the winter season operational mode. During the winter, the heat pump gains thermal energy from the working fluid extracted from the hot aquifer (left-hand side reservoir) to provide space heating. Once out of the heat pump, this colder fluid is injected into the cold aquifer (right-hand side reservoir). During the summer, the heat pump is run in reverse to provide space cooling and thermal energy is transferred to the cold extraction fluid. This is then injected into the hot well for storage until the winter. The thickness of the permeable layer h is constant. The fluid front r of the working fluid is time dependent. In the hot aquifer, the diffusion front is indicated and shows the approximate volume of rock in thermal contact with the fluid.

The volume of the surrounding rock is defined as $V_r = A_f L$, where L is the diffusion length given by $\sqrt{K_r \tau_{cyc}}$ where the cycle time is τ_{cyc} and K_r is the thermal diffusivity. A_f is the maximum surface area of the working fluid.

In each aquifer, we model the exchange of thermal energy between the injected fluid and the surrounding rock, using the heat transfer coefficient λ , acting over the surface area A_f . The temperature of the system is written in dimensionless form, such that $\theta = \Delta T_s T + T_0$, where T_0 is the initial ambient temperature of the subsurface and ΔT_s is the change in temperature from the heat pump system in the summer. For the hot aquifer, undergoing constant injection of fluid with volume flux Q during the summer season, $0 < t < \frac{\tau_{cyc}}{2}$, the conservation of mass and energy in a well-mixed volume requires that

$$\frac{dV_{f_h}}{dt} = Q, \quad (1)$$

$$\frac{dM_{f_h}}{dt} = -\lambda A_{f_h} (T_{f_h} - T_{r_h}) + \rho c_p Q (T_{f_c} + 1), \quad (2)$$

$$\frac{dM_{r_h}}{dt} = \lambda A_{f_h} (T_{f_h} - T_{r_h}). \quad (3)$$

In the above equations, the subscripts h and c refer to the hot and cold aquifers, respectively.

The energy conservation in the cold aquifer, undergoing extraction during the summer, is modelled similarly such that

$$\frac{dV_{f_c}}{dt} = -Q, \quad (4)$$

$$\frac{dM_{f_c}}{dt} = -\lambda A_{f_c} (T_{f_c} - T_{r_c}) - \rho c_p Q T_{f_c}, \quad (5)$$

$$\frac{dM_{r_c}}{dt} = \lambda A_{f_c} (T_{f_c} - T_{r_c}). \quad (6)$$

In the winter, $\frac{\tau_{cyc}}{2} < t < \tau_{cyc}$, the cold aquifer becomes the injection well, and the hot aquifer becomes the extraction well. Equations (3) and (6) remain the same. The thermal mass of the fluid in the hot aquifer is now modelled by

$$\frac{dM_{f_h}}{dt} = -\lambda A_{f_h} (T_{f_h} - T_{r_h}) - \rho c_p Q T_{f_h}. \quad (7)$$

The thermal mass of the fluid in the cold aquifer is now modelled by

$$\frac{dM_{f_c}}{dt} = -\lambda A_{f_c} (T_{f_c} - T_{r_c}) + \rho c_p Q (T_{f_h} - \Delta), \quad (8)$$

where

$$\Delta = \frac{|\Delta T_w|}{|\Delta T_s|}$$

is the ratio of the temperature change of the fluid in the winter to the temperature change of the fluid in the summer.

The fluid volume in each well now changes according to

$$\frac{dV_{f_h}}{dt} = -Q, \quad (9)$$

$$\frac{dV_{f_c}}{dt} = Q. \quad (10)$$

The heat transfer coefficient is defined as $\lambda = \frac{K_r \rho c_p}{L}$ where L is the diffusion distance over a cycle. We have solved the full system in MATLAB and present some analysis of the equations for the long-term behaviour.

2.1 Thermal Loss Ratio

To analyse the thermal loss of the system, we consider the ratio of the maximum fluid volume $V_{f_{\max}}$ to the volume of the rock in thermal contact with the fluid V_r , described by the parameter

$$P_0 = \frac{V_{f_{\max}}}{V_r}.$$

The balance of the fluid volume to the rock volume determines the impact of the thermal energy loss to the aquifer. For $P_0 \gg 1$, such that $V_{f_{\max}} \gg V_r$, the injection fluid only interacts with a small volume of the surrounding rock, and any heat loss is small relative to the thermal mass of the fluid. Conversely, for $P_0 \ll 1$, the fluid is in thermal contact with a large volume of rock, which enhances thermal energy exchange. A similar parameter was first introduced by Doughty *et al.*, and then further developed by Bloemendaal and Hartog, to describe the thermal volume loss to the surrounding rock by the injection fluid (Doughty *et al.* 1982; Bloemendaal and Hartog 2018).

In an axisymmetric system with a cylindrical injection profile where $V_r = (2\pi(r^2 + rh))\sqrt{K_r \tau_{\text{cyc}}}$ and $V_{f_{\max}} = Q \frac{\tau_{\text{cyc}}}{2}$, the parameter P_0 can be expressed as

$$P_0 = \frac{1}{2L \left[\frac{1}{h} + \frac{1}{r} \right]}.$$

It follows that P_0 increases with h , the thickness of the aquifer, or with r , the position of the fluid front at the end of injection. In the following analysis, r is constant, but h may vary.

3. RESULTS

3.1 Balanced systems

We explore this system with an equal amount of energy delivered by the heat pump each season, such that $|\Delta T_s| = |\Delta T_w| = |\Delta T|$. We start with the summer season, when the hot aquifer is initially depleted of the working fluid, and the cold aquifer is full $V_c = V_{f_{\max}}$. Both systems are assumed to have an initial temperature of $T_c = T_h = 0$.

3.1.1 Impact of thermal diffusion

In a perfect scenario where the injection fluid fully retains its thermal energy, we expect both aquifers to reach their respective injection temperature on each cycle. This is modelled by neglecting thermal diffusion, $K_r = 0$, shown in Figure (2a), so the surrounding rock in thermal contact with the fluid is negligible. The aquifer receiving the first injection creates an intrinsic asymmetry. Starting with a hot well injection, this leads to the result $T_h = |\Delta T|$ as initially $T_c = 0$. The following season sees a hot well extraction temperature of $T_h = |\Delta T|$ such that the cold well receives $T_c = T_h - |\Delta T|$. With the heat pump running in an equilibrium, this gives $T_c = 0$, and the cycle repeats. The surrounding rock sees no change in its thermal mass, and $T_r = 0$ at all times. Conversely, starting with a winter season gives a steady state temperature of $T_c = -|\Delta T|$ and $T_h = 0$. The dependency of the injection temperature into each aquifer on the extraction temperature of the alternate aquifer generates a feedback loop. This intrinsic asymmetry impacts the long-term behaviour of the system.

Including thermal diffusion K_r , the exchange of thermal energy between the injection fluid and the surrounding rock results in a shift of the temperature. In Figure (2a), we observe the impact on the temperature profiles of the fluid in the hot and cold aquifers, starting with a summer injection. As K_r increases, heat is transferred to the surrounding rock and lowers the temperature to $T_h < |\Delta T| = 1$, so $T_c < 0$. To illustrate the range of behaviours of the model, we include a calculation using the typical value of $K_r = 10^{-7} \text{ m}^2/\text{s}$. We also show the case of a much larger thermal mass of rock, with an unrealistically large value $K_r = 10^{-3} \text{ m}^2/\text{s}$, to illustrate the case where the thermal energy loss dominates the response of the system. In this scenario, the temperatures of the fluid in the hot and cold aquifers eventually tend to 0.5 and -0.5, respectively. Indeed, in Figure (2a), it is seen that the temperatures tend toward the lower bound $T_c = -\frac{|\Delta T|}{2}$.

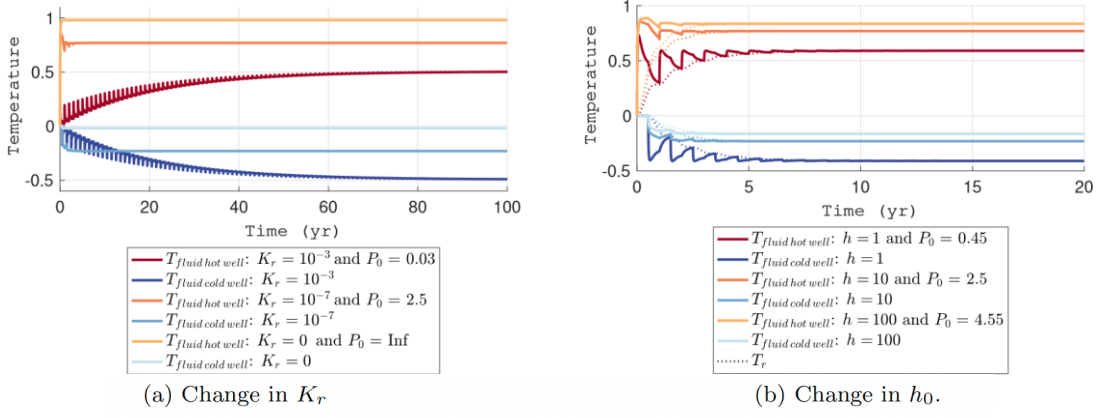


Figure 2: (a) Temperature of the fluid in the hot and cold aquifers over 100 years with varying thermal diffusion coefficients K_r . This results in a varying volume ratio $P_0 = \frac{V_{f_{max}}}{V_r}$. The height of the aquifer is fixed at $h = 10$, and the initial radius $r = 10$. Here $|\Delta T_w| = |\Delta T_s| = 1$. (b) Temperature of the fluid in the hot and cold aquifers for a series of different values of thickness h of the aquifer. The maximum radius $r = 10$, the thermal diffusivity $K_r = 10^{-7}$ and $|\Delta T_w| = |\Delta T_s| = 1$. T_r is the temperature of the surrounding rock in thermal contact with the fluid.

3.1.2 Impact of the ratio of fluid volume to rock volume

The physical geometry of the aquifers impacts the extraction temperature of the working fluid. Smaller values of P_0 result in a greater heat loss to the surrounding rock relative to the injection volume. As the thickness of the aquifer h , increases from very small to very large values, the surface area to volume ratio of the working fluid decreases. Therefore $P_0 = \frac{V_{f_{max}}}{V_r}$ increases, and correspondingly, the thermal energy loss to the surrounding rock, relative to the thermal mass of the fluid, decreases. The calculations in Figure (2b) illustrate the effect of aquifers with different values of P_0 and, hence, vertical extent. Overall, this leads to higher steady-state temperatures, as shown in Figure (3). An analogous trend was observed by Doughty *et al.*, for a single ATES system with constant temperature injection.

As $P_0 \rightarrow 0$, such that $V_r \gg V_{f_{max}}$, the injection fluid interacts with much more of the surrounding rock. The system undergoes large amplitude oscillations during each cycle as relatively more thermal energy is lost to the surroundings. Additional cycles are needed to buffer the larger loss of thermal energy, and this increases the timescale at which the system reaches steady state.

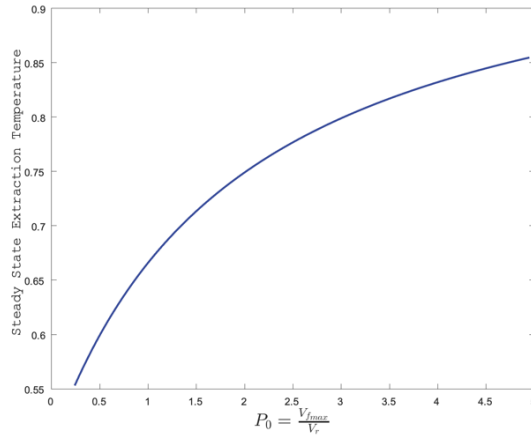


Figure 3: The steady state temperature of the fluid in the hot aquifer for varying P_0 , starting with a summer injection into the hot well. Here $|\Delta T_w| = |\Delta T_s| = 1$.

3.1.3 Difference in temperature of the wells at steady state

As the wells approach steady state, the difference between the hot and cold fluid temperature becomes constant. This steady difference can be derived from equations (1) to (10) as

$$\bar{T}_h - \bar{T}_c = \frac{1 + \frac{|\Delta T_w|}{|\Delta T_s|}}{2} \quad (11)$$

where \bar{T} represents the average fluid temperature over one full cycle. Since we have chosen $|\Delta T_w| = |\Delta T_s| = 1$, in this equilibrium case, we observe all systems tending towards $\bar{T}_h - \bar{T}_c = 1$.

For systems operating in equilibrium, the steady state temperatures of the fluid, T_h and T_c , are dictated by the physical properties of the aquifer, modelled by P_0 , and the heat pump operational constraints $|\Delta T_w|$ and $|\Delta T_s|$. They also depend on which aquifer receives the first injection. The feedback effect of operating well doublets reduces the maximum fluid temperature. With constant injection temperature, a recovery efficiency of 100% corresponds to the extraction temperature matching the initial injection temperature. For constant injection temperatures, this becomes the limiting factor after several cycles (Doughty et al. 1982). In the present model, although the wells reach steady state, and eventually reach a recovery efficiency of 100%, the extraction temperature is smaller than the initial injection temperature owing to the coupling of the wells.

3.2 Imbalanced System

We now explore the case of an imbalanced system, where the winter heat pump extracts more thermal energy from the hot well than the summer heat pump injects into the cold well: $|\Delta T_w| > |\Delta T_s|$. This is likely to occur in buildings facing harsher winter conditions and/or milder summer climates, such as the UK.

In these scenarios, the double well system can develop a gradual draw-down of temperature, as seen in Figure (5). Once the system has locked into a steady decline, the temperature change in each aquifer $\Delta T = T(t = \tau_{cyc}) - T(t = 0)$, over a cycle, may be written as

$$\Delta T = \frac{\Delta V(1 - \Delta)}{V_{f_{h0}} + V_{f_{c0}} + 2\Gamma V_r} \quad (12)$$

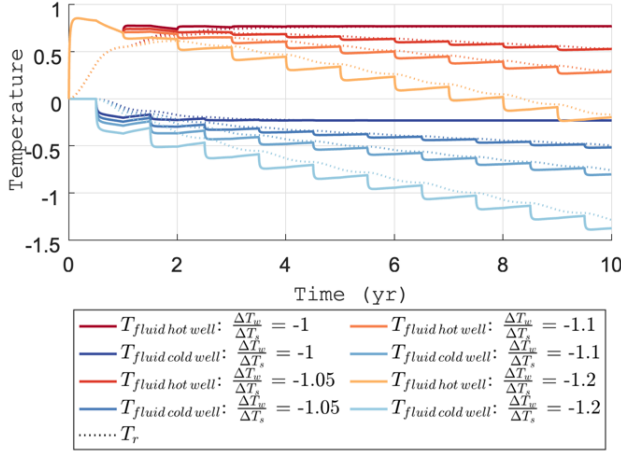


Figure 4: The fluid temperature in the hot and cold aquifers for different imbalanced systems of fixed geometry over ten cycles.

The thermal imbalance of the heat pump $\frac{\Delta T_w}{\Delta T_s}$ changes. The system has thermal diffusivity $K_r = 10^{-7}$, height $h_0 = 10$ and maximum radius $r_0 = 10$. T_r refers to the temperature of the thermal mass of the rock in thermal contact with the working fluid.

Here $V_{f_{h0}}$ and $V_{f_{c0}}$ are the initial fluid volumes at the start of each cycle in the hot and cold aquifers, respectively. The volume injected, or extracted, during each injection cycle is $\Delta V = \frac{Q\tau_{cyc}}{2}$ such that $V_{f_{c0}} = V_{f_{h0}} + \Delta V$. The imbalance between the heating and cooling is modelled by the parameter $\Delta = \frac{|\Delta T_w|}{|\Delta T_s|}$. The parameter $\Gamma = \frac{\rho c_p}{\rho_r c_{pr}}$ and, in the present calculations, for simplicity, we take $\Gamma = 1$. As observed in Figure (4), the larger the thermal imbalance, the greater the temperature drop over time.

3.2.1 Impact of reservoir thermal mass on draw-down

As the thermal mass of the injection fluid decreases (smaller P_0), the system is buffered by the relatively larger thermal mass of the surrounding rock. Hence, a slower rate of decrease in temperature is observed. This is highlighted by equation (12) where,

$$\Delta T \approx \frac{1 - \Delta}{1 + \frac{2\Gamma}{P_0}}$$

and shown in Figure (5).

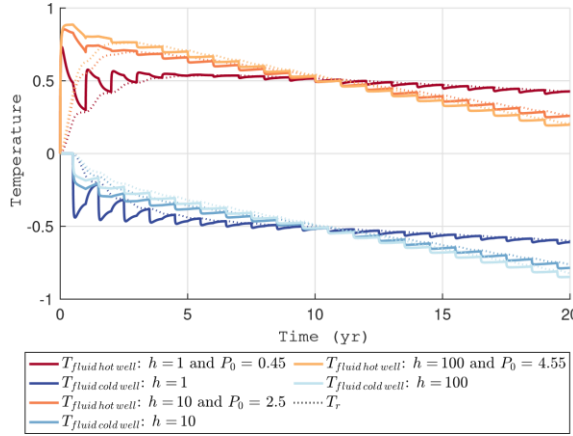


Figure 5: The temperature profile of an imbalanced system with a range of aquifer thickness h over ten cycles. The thermal imbalance of the heat pump is fixed such that $\frac{\Delta T_w}{\Delta T_s} = -1$. The system has thermal diffusivity $K_r = 10^{-7}$ and a maximum radius $r_0 = 10$. T_r refers to the temperature of the thermal mass of the rock in thermal contact with the working fluid.

The long-term behaviour of these systems is highlighted in Figure (6). We observe the temperature gradient once the system has reached its steady decline. The imbalance of the heat pumps has a direct impact on the amount of thermal energy delivered to the system, whereas the physical properties of the aquifers only impact a fraction of this thermal energy. Large systems, with small surface area to volume ratios, suffer the most from the imbalance as the surrounding rock volume is too small to act as an effective thermal energy buffer. This is amplified when there is a large mismatch between the summer and winter heat pump regimes. Larger imbalances, due to the operational settings of the heat pump, have a significant impact on the rate of decline of the system.

4. CONCLUSION

We have presented a simplified model of a double-well ATES system. In equilibrium, where the summer heat supply $Q|\Delta T_s|$ matches the winter demand $Q|\Delta T_w|$, the wells establish a steady temperature difference given by

$$\bar{T}_h - \bar{T}_c = \frac{1 + \frac{|\Delta T_w|}{|\Delta T_s|}}{2}.$$

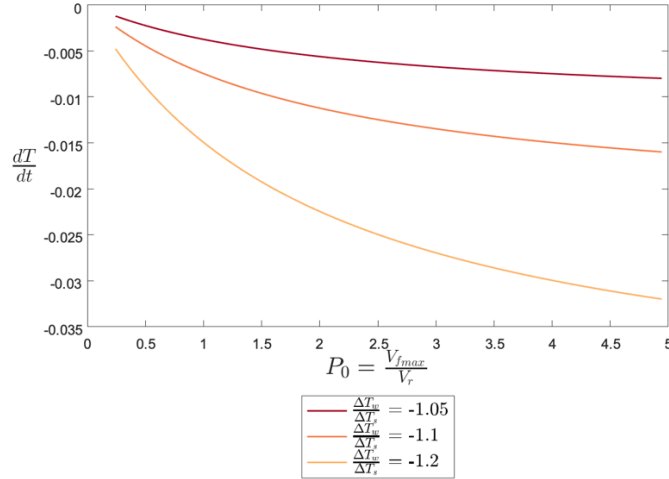


Figure 6: The average gradient of the fluid temperature in the hot aquifer once it has locked into a steady decrease for varying system geometry P_0 . The thickness of the aquifer ranges from $h_0 = 0.5$ to $h_0 = 400$ while the thermal diffusivity $K_r = 10^{-7}$ and maximum radius $r_0 = 10$ are fixed. The three curves show systems operating under different strengths of thermal imbalance.

However, if the heat demand exceeds the cooling-driven heat supply, then the system cools, and the temperature drop scales with

$$\Delta T = \frac{1 - \Delta}{1 + \frac{2\Gamma}{P_0}}.$$

The rate of cooling increases as the thermal mass of rock in contact with the fluid decreases. This suggests that radially extended short reservoirs ($h \ll 1$), as well as vertically extended thin reservoirs ($r \ll 1$), buffer the cooling effect.

We note that the modelling in this paper has been simplified in order to facilitate insight and understanding of the system's overall behaviour. In further work (Lepinay and Woods 2024), we have developed a full numerical simulation of the heat conduction from the well into the neighbouring host rock, including both the spatial and temporal evolution of the temperature field in a double well system. The results of the full simulation are consistent with the results of the idealised model presented herein.

In designing a double aquifer thermal energy storage system in the UK, the initial deployment of the system may be based on winter heating. As the surface cooling infrastructure develops, the installation of a summer heat supply to match the demand may be installed at a later stage. The present modelling enables the calculation of the cooling rate of the system prior to sufficient thermal recharge being installed. As such, the penalty in heating efficiency of any mismatch in the system can be assessed. We are presently exploring the use of this modelling approach to develop a perched aquifer in Cambridge for initial use as a heat source for surface heat pumps, but with a longer-term plan to recharge the system through solar collection in summer.

REFERENCES

- Bloemendal, Martin, and Niels Hartog. 2018. 'Analysis of the Impact of Storage Conditions on the Thermal Recovery Efficiency of Low-Temperature ATES Systems'. *Geothermics* 71 (January): 306–19.
- Bloemendal, Martin, and Theo Olschoorn. 2018. 'ATES Systems in Aquifers with High Ambient Groundwater Flow Velocity'. *Geothermics* 75 (September): 81–92.
- Bödvarsson, Guðmundur S., and Chin Fu Tsang. 1982. 'Injection and Thermal Breakthrough in Fractured Geothermal Reservoirs'. *Journal of Geophysical Research: Solid Earth* 87 (B2): 1031–48.
- Bonte, Matthijs, Pieter Stuyfzand, Adriana Hulsmann, and Patrick Van Beelen. 2011. 'Underground Thermal Energy Storage: Environmental Risks and Policy Developments in the Netherlands and European Union'. *Ecology and Society* 16 (1).
- Doughty, Christine, Göran Hellström, Chin Fu Tsang, and Johan Claesson. 1982. 'A Dimensionless Parameter Approach to the Thermal Behavior of an Aquifer Thermal Energy Storage System'. *Water Resources Research* 18 (3): 571–87.
- Eggen, Geir, and Geir Vangnes. 2005. 'Heat Pump for District Cooling and Heating at Oslo Airport Gardermoen'. In *Proceedings 8th IEA Heat Pump Conference, Las Vegas, Nevada*. Vol. 30.
- Fleuchaus, Paul, Simon Schüppler, Bas Godschalk, Guido Bakema, and Philipp Blum. 2020. 'Performance Analysis of Aquifer Thermal Energy Storage (ATES)'. *Renewable Energy* 146 (February): 1536–48.
- Schout, Gilian, Benno Drijver, Mariene Gutierrez-Neri, and Ruud Schotting. 2014. 'Analysis of Recovery Efficiency in High-Temperature Aquifer Thermal Energy Storage: A Rayleigh-Based Method'. *Hydrogeology Journal* 22 (1): 281–91.
- Sommer, Wijb, Pieter Doornenbal, Benno Drijver, P. Gaans, Ingo Leusbroek, Tim Grotenhuis, and Huub Rijnaarts. 2013. 'Thermal Performance and Heat Transport in Aquifer Thermal Energy Storage'. *Water Resources Research* 22 (February): 1–17.
- Sommer, Wijb, Johan Valstar, Pauline van Gaans, Tim Grotenhuis, and Huub Rijnaarts. 2013. 'The Impact of Aquifer Heterogeneity on the Performance of Aquifer Thermal Energy Storage'. *Water Resources Research* 49 (12): 8128–38.
- Willemse, N. 2016. 'Rapportage Bodemenergiesystemen in Nederland'. *RVO/IF Technology, Arnhem* 686.